

**NASA TECHNICAL  
MEMORANDUM**

NASA TM X-52261

NASA TM X-52261

FACILITY FORM 602

N67 17828

(ACCESSION NUMBER)

(THRU)

39

(PAGES)

1

(CODE)

TMX-52261

(NASA CR OR TMX OR AD NUMBER)

03

(CATEGORY)

**PRELIMINARY EXPERIMENTAL EVALUATION OF  
A BRAYTON CYCLE TURBOCOMPRESSOR  
OPERATING ON GAS BEARINGS**

by Robert Y. Wong, Robert C. Evans,  
and Donald J. Spackman  
Lewis Research Center  
Cleveland, Ohio

GPO PRICE \$ \_\_\_\_\_

CFSTI PRICE(S) \$ \_\_\_\_\_

Hard copy (HC) 3.00

Microfiche (MF) .65

ff 653 July 65

**PRELIMINARY EXPERIMENTAL EVALUATION OF A BRAYTON CYCLE  
TURBOCOMPRESSOR OPERATING ON GAS BEARINGS**

**by Robert Y. Wong, Robert C. Evans, and Donald J. Spackman**

**Lewis Research Center  
Cleveland, Ohio**

**NATIONAL AERONAUTICS AND SPACE ADMINISTRATION**

PRELIMINARY EXPERIMENTAL EVALUATION OF A BRAYTON CYCLE

TURBOCOMPRESSOR OPERATING ON GAS BEARINGS

By Robert Y. Wong, Robert C. Evans, and Donald J. Spackman

Lewis Research Center

SUMMARY

E-3752

As part of a technology program on Brayton Cycle Space Power Systems a turbocompressor for a reference two shaft system operating on gas bearings was designed and built, under contract, to operate on argon. Upon delivery a preliminary exploratory evaluation of the turbocompressor was made to reveal packaging and operating problems which are a result of integrating gas bearings and turbomachinery into a single package. These problems include maintaining a film thickness near 0.0005 inch in order to avoid rotor contact due to overload or instability and maintaining moderate bearing temperatures for maximum life, and flexibility to accommodate differential thermal growth as affected by heat from the turbine and bearings.

The gas bearings have been operated as self-acting on argon at the design speed of 38,500 rpm. The turbine has been operated in argon with inlet temperatures of up to 1000° F. Critical speeds appear within the range of 2000 to 20,000 rpm. Two criticals, 5500 and 8000 rpm, have been identified as the first and second rigid body criticals. Internal temperature measurements indicate a lack of sufficient thermal isolation between the turbine working fluid and the internal parts. The higher than design bearing temperatures could reduce the expected life of the pivots. Strain gage bearing load sensors showed a substantial loss in journal bearing load. However, the confidence level in the strain gages is very low because of the thermal gradients which they are subjected to and because they are designed to operate under isothermal conditions. Furthermore, calculations of differential growth do not support the strain gage indications of load loss.

Three problem areas appear to require attention. They include the apparent threshold of a critical speed at the design speed of 38,500 rpm, the possibility of insufficient thermal isolation between the turbine inlet and the internal parts, and the need for a means of obtaining a reliable indication of journal bearing load.

These results indicate that modifications are needed to improve the thermal isolation between the turbine and the internal parts and to sense journal bearing load. Other modifications to be made include an increase in the preload of the journal bearings, a reduction in the spring rate of the loading diaphragms and a means to pneumatically vary the journal bearing load.

## INTRODUCTION

The Lewis Research Center is currently engaged in a technology program to study components for Brayton Cycle Space Power Systems. As part of this program, a 10 KW-two shaft Solar Brayton System using argon as the working fluid was selected as a reference system for further study (ref. 1). Figure 1 shows a schematic diagram of the reference two shaft system. Components for this system are being procured under contract for ground system evaluation at the Lewis Research Center.

For a space power system, it is desirable to use bearings lubricated with cycle gas and that the rotating components on a common shaft be contained in one housing. This provides compactness, greatly simplifies the shaft sealing problem, and eliminates the need for an external lubrication system.

As part of the technology program a turbine compressor with gas bearings on a common shaft for the reference system was designed, fabricated under contract, and delivered for evaluation. This turbine-compressor is shown in figure 2 and was designed for an argon weight flow of 0.611 lbs/sec. The compressor was designed for a total pressure ratio of 2.3 while the turbine was designed for a total pressure ratio of 1.56. The journal bearings are designed with self-acting pivoted pads using three sectors and for argon lubrication. The compressor side of the thrust bearing includes eight self-acting stepped pads. For start-up and shutdown, bearing lubrication is maintained with external pressurization.

The integration of a 1500° F turbine with a moderate temperature compressor and gas bearings that require isothermal conditions and moderate operating temperature into a single unit presented the problem of maintaining a lubrication film thickness of 0.0005 inch to prevent contact between the shaft and shoes. Thermal barriers to provide thermal isolation and heat shunts to provide isothermal conditions are incorporated into the design. In addition a flexible mounted shoe is used to accommodate differential thermal expansion.

Upon delivery of the turbocompressor a preliminary exploratory study was made of mechanical and dynamic behavior of the delivered hardware as affected by rotor speed and turbine heat. The experimental investigation consisted of slowly varying speed, weight flow, and turbine inlet temperature while observations of shaft motions, internal temperature distributions, and mechanical reactions to expansion were made. The turbine-compressor was tested with turbine inlet temperatures up to 1000° F and speeds up to 38,500 rpm with gas bearings operating as self-acting and externally pressurized lubrication.

Included in this report are descriptions of the test and apparatus together with observations and results. Included also are modifications to be made as a result of this investigation.

## SYMBOLS

|                |   |   |
|----------------|---|---|
| c              | bearings clearance (difference between bearing and journal radii) | in.   |
| P <sub>a</sub> | ambient pressure  | lbs/in <sup>2</sup> -abs                            |
| R              | journal radius  | in.   |
| Ω              | angular velocity  | Radians/sec   |
| λ              | bearing compressibility number                                    | $\frac{6\mu\Omega}{P_a} \left(\frac{R}{c}\right)^2$ |
| μ              | lubricant viscosity   | lb/sec-in <sup>2</sup>                              |

## TURBO-COMPRESSOR DESIGN CONDITIONS

The design conditions for the subject turbo-compressor package are as follows:

## Turbomachinery

|                                  |        |
|----------------------------------|--------|
| Working fluid                    | Argon  |
| Mass flow rate, lb/sec           | 0.611  |
| Turbine inlet temperature, °R    | 1950   |
| Turbine inlet pressure, psia     | 13.2   |
| Turbine total pressure ratio     | 1.56   |
| Compressor inlet temperature, °R | 536    |
| Compressor inlet pressure, psia  | 6.0    |
| Compressor total pressure ratio  | 2.3    |
| Speed, rpm                       | 38,500 |

## Gas Bearings

|                                      |       |
|--------------------------------------|-------|
| Working fluid                        | Argon |
| Ambient temperature, °F              | 500   |
| Ambient pressure, psia               | 12    |
| Bearing number, λ (journal bearings) | 1.5   |

## TURBO-COMPRESSOR PACKAGE DESCRIPTION

The turbo-compressor as designed to meet the design conditions listed in the previous section is shown in sectional view in figure 3. The radial inflow turbine and centrifugal compressor are mounted on the ends of a common shaft with two journals and a thrust runner between them. Each journal bearing includes three self-acting pivoted pads using argon for lubrication. The compressor side of the thrust bearing is designed using eight self-acting stepped pads with argon gas for lubrication. The self-acting gas bearings are provided with external pressurization for lubrication during start and shutdown. The turbine side of the thrust bearing

is a plain externally pressurized bearing. A more complete description of the components will follow.

### Turbine

A photograph of the turbine with the inlet scroll and rotor housing removed is shown in figure 4. The turbine rotor has a diameter of 6.02 inches at the inlet and 4.29 inches at the outlet. There are eleven rotor vanes and eleven splitter vanes. The splitter vanes are used to reduce the gas loading on the inlet portion of the rotor vanes. The stator consisted of 14 vanes which are fabricated as integral parts of the inlet scroll and rotor housing. Aerodynamic design information, including the velocity diagrams and blade surface velocities may be found in reference 2.

### Compressor

A photograph of the compressor with the outlet scroll and rotor housing removed is given in figure 5. The compressor rotor has a diameter of 3-1/2 inches at the inlet and 6 inches at the outlet. There are 15 vanes on the rotor and 23 vanes in the diffuser.

### Journal Bearings

The journal bearings are designed with self-acting pivoted pads, each with four orifices for external pressurization as shown in figure 6-a,b. The pivot is located 65 percent of the pad length from the leading edge. The journal bearing pad and shaft surfaces and the pivot ball and socket surfaces are tungsten carbide. The pivots are designed using sliding contact between ball and socket. Four orifices are used in each pad for external pressurization for lubrication during start and shutdown. As shown in figure 6 c, the balls for two of the pads are mounted rigidly while the ball on the third pad is mounted on a flexible diaphragm with a nominal spring rate of 4000 lbs/in. The diaphragm allows the journal bearing to be pre-loaded to maintain stability, and the flexibility of the diaphragm allows the bearing to accommodate some differential growth due to thermal effects.

### Thrust Bearings

During normal operation the net thrust on the rotor is toward the compressor. Therefore, a self-acting bearing was designed to control the thrust in this direction. The self-acting thrust stator is a Rayleigh-stepped bearing with eight lands as shown in figure 7. Alternate lands are provided with external pressurization orifices (a total of four orifices). This external pressurization capability is provided for use during start-up and shutdown to prevent accidental rubbing, even though the thrust is normally toward the turbine during these maneuvers.

For start-up and shutdown, an externally pressurized thrust stator is provided to accommodate thrust toward the turbine. A total of six ori-

fices are used.

The thrust runner surfaces are coated with tungsten carbide. The two thrust stators are rigidly mounted together. The stator assembly is mounted in a gimbal assembly as shown in figure 8 which allows the stators to pivot in all directions. The gimbal assembly allows the thrust stator assembly freedom to follow any excursions that the thrust runner may go through as well as changes in mount geometry due to thermal growths.

### Mechanical Design

Shown in figure 9 are the mechanical design features used to control the internal temperature of the package. Thermal isolation between the hot turbine and the rest of the package is obtained by the use of extended heat paths such as bellows on outer housing, radiation shielding with surfaces of low emissivity, minimum cross-sectional areas to heat flow, and high resistance heat paths such as curvic couplings and bolted flanges. Isothermal conditions, where required, are approached by the use of copper heat shunts as shown in figure 9.

The heat generated by the self-acting journal bearings and heat flowing from the turbine are removed by a cooling flow (up to 1.0 percent of the system flow) and by the use of the compressor rotor as a heat sink. The cooling flow is bled from the compressor and cooled with a heat exchanger to 100° F before it is brought into the journal bearing cavities. The cooling gas flows over the journal pads and leaves the bearing cavity through the labyrinth seals to be discharged into the turbine and compressor flows as shown in figure 9.

## APPARATUS AND PROCEDURE

### Test Loop

The test loop, as designed, is shown in figure 10 where it can be seen that the turbine and compressor were intended to be operated in separate loops, the turbine in argon and the compressor in air. With this facility tightly sealed, turbine inlet temperature of 1500° F are possible.

Tracing the argon flow through the loop, starting with the inventory control which varies the amount of argon in the system depending on the operating conditions of the loop, the argon is first passed through the facility compressor which raises the pressure of the argon to the desired level. The facility compressor is provided with controls including the outlet pressure control and the critical flow nozzle. Since the facility compressor operates at subatmospheric conditions, it is provided with shaft seals that must be buffered with argon in order to prevent contamination of the argon with air. In order to minimize the argon buffer gas usage, a buffer seal gas system is used to recirculate the buffer gas that leaks into the facility compressor. The buffer gas that leaks from the facility compressor must be replaced. This is another function of the inventory

control. The critical flow nozzle and the compressor outlet pressure control are used to assure that the facility compressor outlet pressure is maintained constant. The critical flow nozzle is of the venturi type with a diffuser that has a recovery coefficient of 0.9.

Next, the flow passes through the heater where it is heated to the desired temperature level. From the heater the flow passes through a 2 micron filter. The filter was installed as a precautionary measure to reduce the possibility of dust particles working their way into the gas bearings and thereby causing a bearing failure.

From the filter the flow is split between the turbine and the turbine inlet pressure control valve. The valve is used to maintain the desired pressure at the turbine inlet by passing a portion of the flow around the turbine. Flow from the filter passes through the turbine where power is extracted and then through the turbine speed control valve which varies the power output of the turbine to maintain the desired speed.

From the turbine speed control valve the flow then passes through the cooler before it begins the cycle again. Bellows, as shown in figure 10, with a spring rate of approximately 45 lbs/in. were used between the piping and the package to minimize piping loads due to thermal expansion on the package.

For the research compressor, air flow from the Lewis Pressurized Air Facility first passes through an absolute pressure regulator before going to the research compressor. From the compressor the air is discharged through a throttle valve in the Lewis Altitude Exhaust Facility.

By controlling the pressure level that the research compressor operates at, it is possible to control its power requirements.

#### Air Tests

Due to mechanical difficulties with the facility compressor, it was decided to do the initial testing using air through the turbine rather than argon. This eliminated the immediate need for the facility compressor and resulted in the modified test loop as shown in figure 11.

This loop is the original loop minus the facility compressor and its controls. The air enters from the Lewis pressurized air system and is controlled by a pressure regulator valve. The flow is through the loop as in the original design except that after leaving the cooler the air is exhausted to the room. The use of air in the test apparatus which was designed to operate with a facility compressor and argon as the working fluid imposes a limit on the turbine inlet temperature that can be achieved in this test. This results from the fact that the facility compressor had a discharge temperature of 500° F whereas the facility air is at room temperature of about 80° F. Further, air has a specific heat of twice that

of argon. Which means for the same energy input, the temperature increase of the air is only half that of the argon. With this arrangement, hereafter called Test 1, it was necessary to operate the compressor at .5 psia and turbine inlet conditions of 20 psia and 500° F to get a speed of 38,500 rpm in the package. This was the maximum turbine inlet temperature with full heater output.

The first series of tests was conducted with the thrust bearings externally pressurized with argon and the journal bearings in self-acting mode of operation on argon. In order to continue the air test to higher temperatures, it was necessary to reduce the turbine weight flow. This was accomplished by operating the turbine at subatmospheric pressures and at higher pressure ratios than the first test to permit higher turbine inlet temperatures without exceeding operating limits with air. Trace heaters were placed on the pipes upstream of the heater and between the heater and turbine to further increase the turbine inlet temperature. For this series of tests, the heater was limited to a temperature of 1200° F to prevent oxidation and scaling. This resulted in a turbine inlet temperature of 870° F. Reduced pressure was achieved by discharging the air into the Lewis Altitude Exhaust System rather than the room as in Test 1. The loop diagram for Test 2 is shown in figure 12. The remaining apparatus is the same as in Test 1. Details of the test will be given in a later section.

#### Argon Tests

With the difficulties in the facility compressor corrected the hot loop using argon was used as shown in figure 10.

Hereafter this test shall be called Test 3. The loop operates exactly as was designed and was discussed earlier. Due to thermal cycling, leaks opened in some of the loop expansion joints and were bad enough to contaminate the loop argon with 5 to 10 percent air. This, of course, posed the problem of oxidation and scaling in the heater. Since the leaks were so difficult to repair without complete disassembly it was decided to proceed at a reduced temperature. A limit of 1300° F was set upon the heater which limited the turbine inlet temperature to 1000° F. Details of the test will be discussed in a later section.

A photograph of the test facility with the facility compressor is given in figure 13 and a photograph of the turbo-compressor installation is shown in figure 14.

#### INSTRUMENTATION

The instrumentation used to measure and record the performance of the turbocompressor in the three tests are as follows.

Chromel-Alumel thermocouples were used to measure all temperatures. Turbine inlet temperatures were measured by a bare spike total temperature rake located approximately 2 inches upstream of the turbine inlet scroll

flange. Internal package temperatures used for thermal mapping were measured with bare spike thermocouples spot welded to internal parts of the package. Fifty-four thermocouples were used for this purpose. The location of these thermocouples can be seen in the Figure given with table I. Two or more thermocouples were located at critical temperature points such as those in the bearing areas.

Strain gage type pressure transducers were used to measure system pressures. Static taps and total pressure probes were located 2 inches upstream and downstream of the turbocompressor inlet and outlet, respectively.

The journal bearing loads were measured using weld type bonded wire strain gages. These gages were welded to the bearing diaphragm in a four arm bridge configuration as shown in figure 15.

The speed was measured with a high temperature magnetic-type pickup. Six magnetic blocks were imbedded in the shaft for this purpose. The frequency output was fed into an electronic frequency counter.

All temperatures, pressures, speed, and bearing loads were recorded on strip chart potentiometers. At selected intervals in time, temperature, pressure, and speed, data was recorded by an automatic data recorder and processed through a digital computer.

The shaft motions were measured using capacitive proximity instrumentation consisting of non-contact sensing probes and high frequency oscillator-amplifiers. A change in distance between the sensing probe and the sensed object, in this case the shaft or the thrust bearing runner, gives a proportional change in capacitance which in turn changes the amplifier output voltage. A total of six probes was used to measure the operating characteristics of the bearings as shown in figure 16. Two probes were located in close proximity to the compressor journal bearing. The probes were placed approximately .004 inches from the shaft surface and located 90° apart to give the x and y axis movements of the shaft relative to the housing.

Two probes were located approximately .004 inches from the shaft surface in close proximity to the turbine journal bearing. The probes measuring the x axis displacement of the compressor and turbine journal bearings are located in the same plane. The probes measuring the y axis displacement are also located together in the same plane.

Two probes were used to measure the gas film thickness between the thrust bearing stators and the thrust runner. The probes were mounted on the thrust stator directly opposite each other.

The displacements from all capacitive instrumentation were continually monitored on dual beam oscilloscopes and at the same time recorded along with the speed on an FM magnetic tape recorder. This data was played back

and filmed after each test and the dynamic characteristics were then analyzed by frame-by-frame projection using a photo-optical analyzer.

### TEST PROGRAM AND RESULTS

During all three tests the bearings were operating with argon, and the compressor was operating on air at all times. The turbine was operated as follows: Test 1-Turbine inlet temperature of 500° F with air, Test 2-Turbine inlet temperature of 800° F with air, and Test 3-Turbine inlet temperature of 1000° F with argon. Each test consisted of gradually varying speed, flow rate, and turbine inlet temperature while observations were made of shaft motions, temperature distributions, and package reactions.

#### Test 1-Turbine Inlet Temperature of 500° F

In its first test, the package was run at the contractor's facilities for 5 hours with the turbine and compressor operating in air, while the journal bearings were operated self-acting and the thrust bearings were operated externally pressurized. The first inhouse test would duplicate this test.

The purpose of duplicating this test was to:

1. Obtain the operating characteristics of the delivered gas bearings.
2. To assure that the package did not sustain damage during shipment.

This inhouse test is shown in figure 17 where speed (rpm), turbine inlet temperature (°F), and compressor and turbine journal load (lb) are plotted against time (hr). From the Figure it can be seen that the package was started with external pressurization and speed is negative at approximately 200 rpm. The speed was brought up to 38,000 rpm in steps. Shortly after reaching 38,000 rpm there is a rapid drop in speed due to a malfunction in a control circuit causing an automatic shutdown.

After correcting the fault, the package was restarted and brought to 38,000 rpm. Upon placing the journal bearings into self-acting operation, the speed was maintained between 38,000 and 38,500. The plot of turbine inlet temperature shows a rapid rise from room temperature to about 300° F. From 300° F the turbine inlet temperature is gradually brought up to about 500° F. The dip in temperature at about 2 hours was caused by the automatic shutdown. In the plot of indicated bearing loads only the compressor end journal is shown for the complete test while the turbine end journal is shown only for self-acting operation because the turbine data for the remainder of the run was misplaced. However, as will be seen from subsequent tests, the indicated turbine journal bearing load behaves in a manner similar to the indicated compressor load curve shown. It should be noted, the term "indicated turbine and compressor journal bearing load" is used because of the low level of confidence in the strain gages when

they are subjected to temperature gradients. During the following discussion this should be kept well in mind so that the discussion would not be misleading.

From the indicated compressor journal bearing load curve, it can be seen that the load is fairly steady until the unit is accelerated. There is a small rise in load as the unit is accelerated to 38,000 rpm and then the indicated load falls rapidly with decrease in speed and increases with speed as it is accelerated after the shutdown. From the peak indicated load, there is a trend of decreasing load with time. Further, as the journal bearings are placed in self-acting operation (external pressurization removed), there is about a 3 lb drop in load. Under self-acting journal bearing operation there is a continued gradual drop in load until external pressurization is returned and there is a continued gradual drop in load until external pressurization is returned and there is an associated increase in load of about 3 lbs. From figure 17 it can be seen that the journal bearings were operated under self-acting conditions for about one hour.

Throughout the test the temperature distribution within the package and the radial and axial excursions of the shaft were monitored and recorded and will be discussed in a subsequent section.

#### Test 2-Turbine Inlet Temperature Increased to 800° F

The purpose of this test was to operate the package with a turbine inlet temperature significantly above the previous test to determine how temperature distributions change as the turbine inlet temperature is increased and to determine the package reaction to higher temperatures.

This test was similar to Test 1 which was limited to a temperature of 500° F by heater output and turbine weight flow. In order to achieve an increase in turbine inlet temperature the turbine weight flow was reduced by reducing the turbine inlet pressure and discharging the turbine exhaust into the altitude exhaust system. In order to prevent scaling within the loop due to operation in air, the heater was limited to 1200° F. This limited the turbine inlet temperature to about 800° F. This precaution was taken because of the possibility of scale particles finding their way into the bearings and causing a bearing failure.

A plot of speed (rpm), turbine inlet temperature (°F), and indicated turbine and compressor journal bearing load as a function of time (hr) are plotted in figure 18 for this run.

Although not shown, the speed was maintained at about 2000 rpm while the turbine inlet temperature was being brought up to 375° F by the heater. At a turbine inlet temperature of 375° F the speed of the package was brought up to 35,000 rpm rapidly. From 35,000 rpm the speed was gradually increased to 38,000 rpm. The dips in speed in going to 38,000 were caused by changes in compressor and turbine operating condi-

tions. The change in compressor and turbine operating conditions were made to achieve changes in turbine inlet temperature. The turbine inlet temperature was gradually increased to 825° F. As in the previous test the indicated load rises as speed is increased then drops rapidly with time. It is seen that the indicated turbine load drops more rapidly at first than the indicated compressor load. The dips in the indicated load curves between 1/2 hour and 1-1/2 hours occurred when cooling flow rate and/or cooling flow temperature was varied. The dips in the indicated load curves between 1-1/2 hours and 2-1/2 hours are caused by the dips in speeds. During this period the normal thrust bearing external pressurization was reduced to about 1/2 and the cooling flow temperature and cooling flow rate adjusted to stem the trend of indicated load loss. With the indicated loads at 9-1/2 pounds and 8-1/2 pounds for the turbine and compressor end journals, respectively, the transition to self-acting operation in the journals was begun and it can be noted that the indicated load drops 2 pounds rapidly as the external pressurization is cut off. At the completion of the transition the compressor indicated load is down to 6-1/2 pounds while the turbine indicated load is up to 10-1/4 pounds. During self acting operation the indicated turbine load drops to 7 pounds while the indicated compressor load gradually rises to 7 pounds then falls back to 6-1/2 pounds. In the transition back to external pressurization the indicated turbine journal load recovers 4 pounds while the indicated compressor journal bearing load recovers 3-1/2 pounds. The recovery in load is followed by a rapid decrease in load and then is followed by another sharp rise in the indicated turbine journal load in a lesser rise in the compressor load, as the turbine inlet temperature is reduced. Then as speed is reduced the load falls off again.

As in the previous test the internal temperature distribution of the package and the radial and axial motion of the shaft were monitored and recorded and will be discussed in a subsequent section.

### Test 3-Turbine Inlet Temperature Increased to 1000° F

The purpose of this test was to obtain the internal temperature distribution and package mechanical reaction to still higher turbine inlet temperatures. This was done by taking advantage of the lower specific heat of argon to get higher temperatures. Because of subatmospheric operation, air leakage into the loop amounts to 5 to 10 percent of the argon and again posed the problem of scaling within the loop. Since the concentration of air for this test was lower than the previous test the limit on heater temperature was increased to 1300° F.

Figure 19 presents the variation in speed (RPM), turbine inlet temperature (°F), and indicated load in the compressor and turbine journal bearing with time (hr.) for Test No. 3. Similar to Test No. 2 the speed was maintained at about 2000 until the turbine inlet temperature reached 400° F. The speed was raised to 20,000 and held for 10 minutes and then raised to 38,000. The dips in speed are again caused by changes in compressor and turbine operating condition, to achieve changes in turbine weight flow and therefore changes in turbine inlet temperatures. From

400° F the turbine inlet temperature is gradually brought up to 1000° F. The indicated load in the compressor and turbine journal bearings show that the indicated turbine end journal bearing load drops off initially to 9.7 pounds and then recovers and levels off at about 12-1/2 pounds while the indicated compressor end journal bearing load drops off to about 7-1/2 pounds and levels off. No attempt was made to make the transition into self-acting operation in the journal bearings because there is a 3 pound loss in load in making this transition. A 3 pound loss would reduce the compressor journal bearing load to 4.5 pounds which is very near the threshold of whirl.

The cooling and external pressurization conditions used in Test No. 2 were set to stem the trend of indicated load loss. When the load finally leveled out at about 2 hours the cooling flow rate, cooling flow temperature, and external pressurization on the normal thrust bearing were varied 30 percent in either direction without significant change in indicated load in either journal bearing.

#### DISCUSSION OF RESULTS

The results obtained from the test program described in the previous section will be discussed as follows: (1) Bearing operating characteristics, (2) Internal temperature distributions, and (3) Indicated loss in journal bearing load.

#### Turbo-Compressor Shaft Motions

The relative radial motions between the rotor and the frame, and relative axial motions between thrust runner and stator were monitored and recorded during testing. Presented in figure 20 are some of the typical radial motions as observed over the speed range investigated. In comparing the shaft excursions for the three tests it was found that the peaks in amplitude when going through the critical speeds shifted not only in magnitude but also in speed. The magnitudes of the peak excursions change as much as 30 percent and the speed changes as much as 2000 rpm. As many as six excursions have been observed within the range from 2000 to 20,000 rpm. In view of these shifts a plot which covers all observed excursions for all three tests is shown for the turbine and compressor journal bearing and the thrust bearing in figure 21(a), (b), and (c), respectively. From figure 21(a) it can be seen that for external pressurization the turbine and journal excursions increase rapidly to a value of  $1.24 \times 10^{-3}$  inches at 5100 rpm. Then as speed is further increased the maximum displacement decreases to  $0.24 \times 10^{-3}$  inches at about 26,000 rpm. From 26,000 to 34,000 rpm the maximum displacement is constant. Between 34,000 and 38,500 rpm the maximum displacement increases from  $0.24 \times 10^{-3}$  inches to  $0.5 \times 10^{-3}$  inches. It can also be seen that for self-acting bearing operation the peak displacements of the excursions are slightly lower than for externally pressurized operation. The rise in displacement indicates that the package is at the threshold of another critical speed or that there is a shift in unbalance of the rotor. The maximum excursion, however, is only  $0.5 \times 10^{-3}$  inches and is considered quite safe at 38,500 rpm.

The slope of the curve at 38,500 rpm indicates that the shaft displacement would increase rapidly above  $0.5 \times 10^{-3}$  inches as speed is increased above 38,500 rpm. This is of concern because accidental overspeeds could result in speed above 38,500 rpm.

The maximum excursions of the compressor end journal as shown in figure 21(b) indicate that the shaft excursion increases as speed is increased above 2000 rpm. The maximum displacement reaches a peak of  $1.44 \times 10^{-3}$  inches at about 8200 rpm. Further increases in speed result in a decrease in the excursions to  $0.18 \times 10^{-3}$  inches at 20,000 rpm. From 20,000 rpm to 31,000 rpm the peak shaft excursion remains at  $0.18 \times 10^{-3}$  inches. From 31,000 to 35,000 rpm there is a slight rise to  $0.21 \times 10^{-3}$  inches where the displacement remains constant to about 38,000 rpm. This slight shift in the curve could mean there is a very slight shift in the unbalance at the compressor end. From 38,000 rpm to 38,500 rpm there is a rise in displacement from  $0.21 \times 10^{-3}$  inches to  $0.32 \times 10^{-3}$  inches.

Further examination of the criticals reveals that the 5100-5500 rpm critical is the conical mode while the critical at 8100-9000 rpm is in the cylindrical mode. These are rigid body criticals and are shown in figure 21(a) and (b) by the cross hatched areas and are labeled the first and second bearing criticals.

Close examination of the other four critical speeds from 2000 to 20,000 rpm failed to reveal any pattern that would lead to their identity. However, they appear to change with operating conditions within the turbine and compressor. Examination of the shaft orbits near 38,000 rpm shows them to be similar to some of the orbits observed at lower speeds. Therefore it is possible that the increases in shaft excursion observed near design speed are harmonic excitations of some of the lower system criticals.

The relative axial motions between thrust stator and thrust runner as shown in figure 21(c) indicates a rise in displacement as the speed is increased above 3000 rpm and reaching a peak of  $0.71 \times 10^{-3}$  inches at 8800 rpm. From 8800 rpm as speed is increased to 20,000 the axial displacement decreases to  $0.23 \times 10^{-3}$  inches. Increasing the speed from 20,000 rpm to 38,500 rpm results in an increase in maximum axial displacement to  $0.26 \times 10^{-3}$  at 32,500 rpm and then a decrease to  $0.24 \times 10^{-3}$  at 38,500 rpm. It should be noted that there are two effects that are superimposed to give the axial excursion indications that are shown. One is the relative axial motion between the shaft and the package and the other is the apparent axial motion which comes from the thrust stator not being able to follow the thrust runner in a wobble motion.

#### Internal Temperature Distributions

The internal temperature distributions observed during the three tests described earlier are tabulated in table I together with temperature distributions predicted by the contractor. Two predictions of temperature distribution were made by the contractor. One was made when the package

was originally designed and a second one was made after the contractor had made some hot runs on a similar package.

From the table it can be seen that the temperature of the internal parts of the package for Test No. 1 are running slightly hotter than Test Nos. 2 and 3. The temperature of the internal parts for all tests are lower than the predicted temperature.

In order to get a common basis for comparison the difference in temperature between a given internal part and the turbine inlet temperature is divided by the turbine inlet temperature and tabulated in table 2 for the last recording of each test and the predicted thermal distributions. Only the last recordings for each test are tabulated because they are the closest to a steady state temperature distribution.

From table 2 it can be seen that the values of temperature difference for Test No. 1 are less than half of the other runs. This means that the parts are running unusually hot for that particular turbine inlet temperature. This further means that there is either excessive heat transfer from the turbine to the internal parts or that heat generation by the self-acting bearings is the major contributor to the temperature of those parts. From the low value of temperature difference 0.049 and 0.068 for the turbine bearing seal holder it can be concluded that there must be excessive heat transfer from the turbine fluids to the internal parts. The high heat transfer comes from the fact that the turbine is being operated in air at high pressure (approximately 20 psia). The other factor in the high internal temperature for Test No. 1 is that the compressor is operating at very low pressure (approximately 0.5 psia) thus minimizing the heat flow from the internal parts to the compressor fluids. Thus it appears that the heat flows into the internal parts from the turbine and is fairly well trapped internally. A further indication of this effect can be seen in Test No. 2 where the turbine inlet pressure reduced to 5.2 psia and the compressor pressure raised to 3.3 psia. These changes in operating conditions tend to reduce the heat transfer from the internal parts to the compressor fluids. For Test No. 2 the difference between the internal parts and the turbine inlet is almost double that of Test No. 1. The temperature difference for the seal assembly is four to five times higher than Test No. 1. Test No. 3 was run with argon in the turbine at 10 psia and air in the compressor at 4.75 psia. This test shows slightly higher temperature differences than Test No. 2. This could be caused by the lower heat generation in the journal bearings due to operation with external pressurization. However, the temperature differences of the turbine seal assembly for Test Nos. 2 and 3 are about equal. This indicates that the heat transfer from the turbine fluids to the internal parts are about the same. Thus the slightly cooler operating temperatures of the internal parts must be attributed to the lower heat generation within the journal bearings.

A comparison of the temperature differences of the test runs and the predictions of the contractor shows that the runs have lower values thus tending to indicate that when the package is run at design temperatures

the internal parts may be overheated. This would indicate that there is a lack of sufficient thermal isolation between the turbine and the internal parts. However, no definite conclusions can be drawn here because of the strong dependence of temperature of internal parts on the operating conditions within the turbine and compressor.

#### Journal Bearing Load

In the three tests described in the earlier section, it was found that after a period of time the indicated load dropped to 6 to 7 pounds under self-acting operation. Journal bearing load is of prime concern for this package because stability of gas bearings is dependent upon maintaining sufficient load. Work done by the contractor had indicated that journal bearing load at about 4 pounds will put the bearing at the threshold of an instability called whirl. Journal bearing load changes can occur in this package if there is differential growth between the shaft and the bearing carrier. Thus, if the bearing carrier temperature rose faster than the shaft temperature as heat soaks in from the turbine, journal bearing load loss can occur.

Analysis of bearing shoe temperatures (assumed to be the same as the shaft temperature) and bearing carrier temperatures in the plane of the pivots for Test No. 2 indicates that the compressor carrier was less than  $10^{\circ}$  hotter than the shaft, while the turbine carrier was as much as  $55^{\circ}$  cooler than the shaft. Thus the temperatures would indicate that the compressor end journal would lose a very small amount of load while the turbine end journal should actually gain some load. Therefore, if there was actually a loss in load as indicated by the strain gages it did not occur because of differential growth between the shaft and carrier. The use of strain gages to indicate load for this application was an unfortunate choice because of the thermal environment that these gages must operate in and of the sensitivity of strain gages to temperature gradients.

Attempts were made to calibrate the strain gages for temperature changes while installed in the package by applying heat to the cooling flow. These calibrations showed a very sharp downward shift in zero as the temperature was applied. With no other means at hand to indicate load the conservative approach was to assume that the strain gauges are giving load values which are lower than the actual load. Thus, when the load indicated by the strain gage indicates the approach of a dangerous condition there should still be some margin of safety available.

#### CONCLUDING REMARKS

The results of a preliminary exploratory study into the mechanical and dynamic behavior of an exploratory Brayton Cycle turbocompressor operating on gas bearings with a turbine inlet temperature up to  $1000^{\circ}$  F and speeds up to 38,500 rpm show the following problem areas:

1. Internal temperature distribution indicates that there is a lack of sufficient thermal isolation between the turbine and the internal parts

of the package, which could cause some over-heating of the internal parts and thus reduce the expected life of such parts as pad pivots and gimbal pivots.

2. Instrumentation provided to sense journal bearing load appears to be of questionable value for this application because of the thermal environment that it must operate in.

3. At the design speed of 38,500 rpm it appears that the package is at the threshold of a critical speed or a harmonic of one of the lower critical speeds. The relative motions between the shaft and pads at this speed are small and are considered safe.

These results indicate that modifications to the turbocompressor are necessary to improve the thermal isolation between the turbine and the internal parts and to incorporate a journal bearing load sensor that will function in the internal environment of this package. Improved thermal isolation will be obtained by reducing the contact or heat flow area between the turbine labyrinth seal and the turbine end journal bearing carrier. Instruments will be provided to sense journal bearing diaphragm deflection. Knowledge of journal bearing diaphragm deflection and diaphragm spring rate will give an indication of journal bearing load provided there is not appreciable thermal gradients on the diaphragm. Another means of sensing journal bearing load is the self-acting film pressure measured from the four external pressurization orifices in each pad. The variation in self-acting film pressure with journal bearing load as affected by speed and ambient pressure, however, will have to be first determined experimentally.

As precautionary measures the preload of the journal bearing will be doubled and the diaphragm spring rate will be reduced to about one-half. This will increase the amount of journal bearing load that can be lost before reaching the threshold of whirl and the reduction in spring rate will reduce the sensitivity of the journal bearing load to differential thermal growth. In addition to these measures a means to vary journal bearing load by pneumatic loading on the diaphragm will also be incorporated to change the load should it become necessary.

#### REFERENCES

1. Bernatowicz, Daniel T.: NASA Solar Brayton Cycle Studies. TP 13-63.
2. Kofskey, Milton G., and Holeski, Donald E.: Cold Performance Evaluation of a 6.02-Inch Radial Inflow Turbine Designed for a 10-Kilowatt Shaft Output Brayton Cycle Space Power Generation System. NASA TN D-2987, 1966.

TABLE 1. - INTERNAL TEMPERATURE DISTRIBUTION  
[Package temperatures, °F]

| Point no. | Test number<br>Part identification                      | 0 M  |      | 1              |                | 2              |                |               | 3              |                |
|-----------|---|------|------|----------------|----------------|----------------|----------------|---------------|----------------|----------------|
|           |   | T    | T    | Time           |                | Time           |                |               | Time           |                |
|           |   | M*   | M**  | 2 hr<br>17 min | 3 hr<br>27 min | 2 hr<br>15 min | 3 hr<br>35 min | 4 hr<br>6 min | 1 hr<br>45 min | 3 hr<br>53 min |
|           | Turbine inlet temperature                               | 1490 | 1490 | 490            | 517            | 706            | 834            | 857           | 800            | 985            |
| 1         | Comp. journ. brg., flex. shoe                           | 400  | 430  | 162            | 323            | 258            | 271            | 272           | 263            | 294            |
| 2         | Comp. journ. brg., fixed shoe                           | 400  | 430  | ---            | ---            | 263            | 275            | 277           | 268            | 300            |
| 3         | Turb. journ. brg., flex. shoe                           | 490  | 550  | 183            | 370            | 300            | 330            | 336           | 282            | 322            |
| 4         | Turb. journ. brg., fixed shoe                           | 490  | 550  | 178            | 369            | 298            | 330            | 335           | 283            | 323            |
| 5         | Turb. end thrust brg.                                   | 510  | 580  | 212            | 372            | 316            | 352            | 356           | 324            | 359            |
| 6         | Compressor end thrust brg.                              | 530  | 580  | 205            | 370            | 318            | 350            | 355           | 326            | 361            |
| 7         | Comp. brg. mount  | 375  | 380  | 150            | 313            | 255            | 258            | 260           | 262            | 295            |
| 8         | Comp. brg. mount  | 410  | 380  | 148            | 312            | 265            | 284            | 287           | 271            | 308            |
| 9         | Comp. brg. mount  | 380  | 370  | 140            | 300            | 248            | 260            | 261           | 254            | 290            |
| 10        | Turb. brg. mount  | 430  | 750  | 190            | 370            | 306            | 340            | 350           | 301            | 353            |
| 11        | Turb. brg. mount  | 415  | 610  | 170            | 350            | 291            | 318            | 325           | 275            | 320            |
| 12        | Turb. brg. mount  | 460  | 510  | 149            | 317            | 267            | 297            | 304           | 269            | 315            |
| 13        | Turb. brg. mount  | 415  | 610  | 156            | 356            | 291            | 323            | 332           | 284            | 334            |
| 14        | Gimbal assembly   | ---  | 510  | 140            | 310            | 269            | 301            | 307           | 273            | 314            |
| 15        | Gimbal assembly   | ---  | 515  | 145            | 319            | 274            | 306            | 311           | 278            | 320            |
| 16        | Gimbal assembly   | ---  | 530  | 140            | 314            | 271            | 305            | 310           | 275            | 317            |
| 17        | Gimbal assembly   | ---  | 560  | 147            | 316            | 273            | 306            | 311           | 280            | 320            |
| 18        | Main frame assembly comp.<br>seal mounting flange       | 400  | 410  | ---            | ---            | 209            | 218            | 218           | 204            | 219            |
| 19        | Main frame assembly comp.<br>brg. carrier mount ring    | 450  | 440  | 138            | 288            | 246            | 281            | 289           | 251            | 289            |
| 20        | Main frame assembly turb.<br>brg. carrier mount ring    | 495  | 500  | 156            | 317            | 261            | 298            | 306           | 269            | 315            |
| 21        | Main frame assembly turb.<br>outer housing mount flange | 900  | 950  | 310            | 411            | 379            | 416            | 429           | 431            | 521            |
| 22        | Longeron  | 750  | 750  | 209            | 339            | 303            | 337            | 345           | 327            | 387            |
| 23        | Longeron  | 510  | 510  | 149            | 292            | 256            | 288            | 294           | 265            | 309            |
| 24        | Longeron  | 500  | 500  | 145            | 288            | 253            | 284            | 290           | 260            | 303            |
| 25        | Longeron  | 470  | 490  | 143            | 284            | 249            | 280            | 285           | 256            | 296            |
| 26        | Longeron  | 460  | 470  | 145            | 281            | 245            | 275            | 280           | 255            | 292            |
| 27        | Longeron  | 440  | 450  | 140            | 275            | 242            | 271            | 276           | 247            | 284            |
| 28        | Longeron  | 430  | 440  | 142            | 272            | 238            | 267            | 271           | 242            | 278            |
| 29        | Longeron  | 425  | 415  | 141            | 268            | 235            | 261            | 264           | 237            | 271            |
| 30        | Turb. seal assembly                                     | 1160 | 1090 | 388            | 469            | 426            | 481            | 495           | 486            | 584            |
| 31        | Turb. seal assembly                                     | 1040 | 1050 | 370            | 451            | 414            | 458            | 471           | 480            | 572            |
| 32        | Radiation shield  | ---  | 870  | 202            | 362            | 316            | 352            | 361           | 326            | 387            |
| 33        | Radiation shield  | ---  | 920  | 198            | 350            | 301            | 332            | 341           | 322            | 384            |

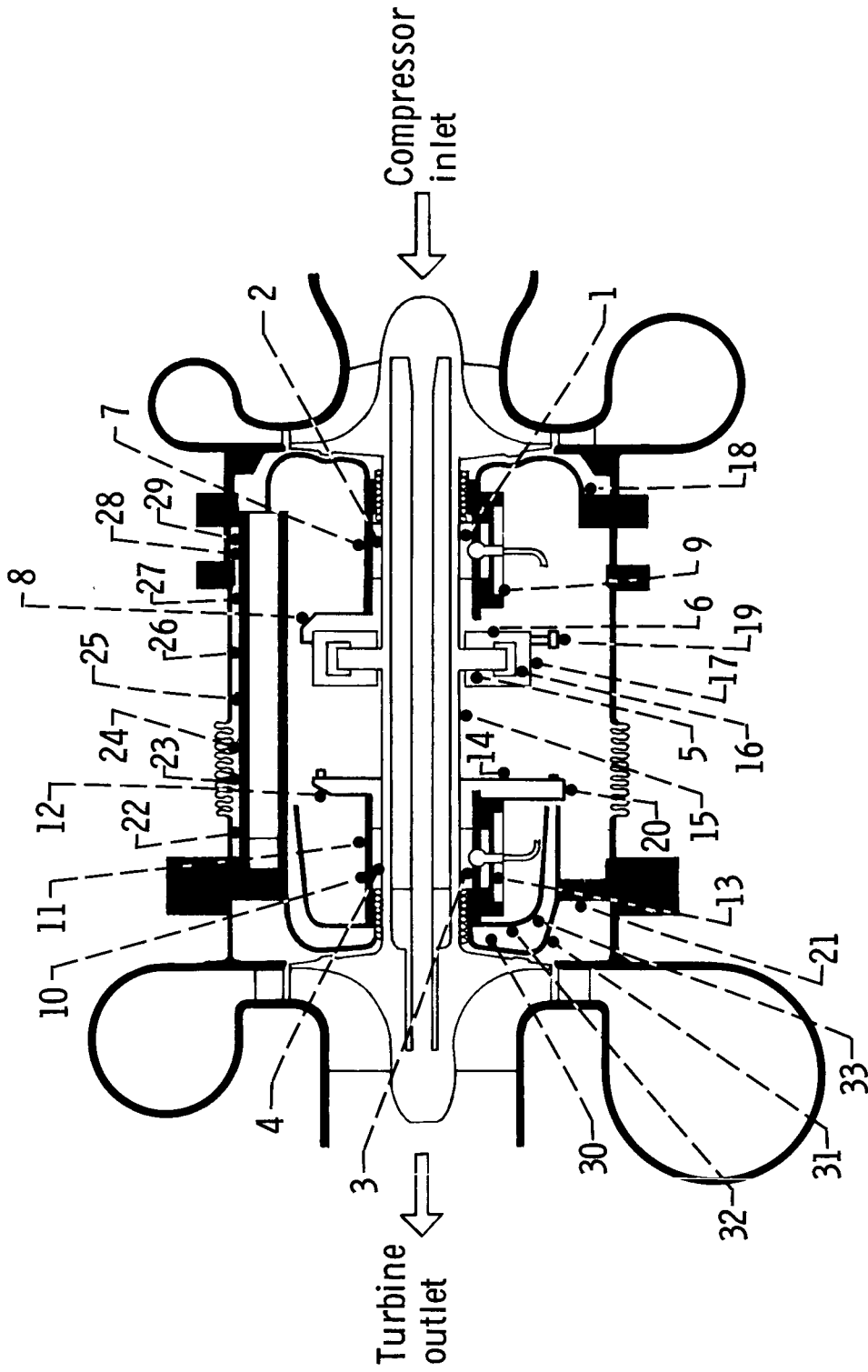
\*Original thermal map  
\*\*Modified thermal map

TABLE 2. - TEMPERATURE DROP BETWEEN TURBINE INLET  
AND INTERNAL PARTS  
[ $\Delta T$ /Turbine inlet temperature]

| Point no. | Test number<br>Part identification                      | 0     | M     | 1              | 2             | 3              |
|-----------|---|-------|-------|----------------|---------------|----------------|
|           |   | T     | T     | Time           |               |                |
|           |   | M*    | M**   | 3 hr<br>27 min | 4 hr<br>6 min | 3 hr<br>53 min |
|           | Turbine inlet temperature, °R                           | 1950  | 1950  | 977            | 1317          | 1445           |
| 1         | Comp. journ. brg., flex. shoe                           | 0.559 | 0.544 | 0.198          | 0.444         | 0.478          |
| 2         | Comp. journ. brg., fixed shoe                           | .559  | .544  | ---            | .440          | .474           |
| 3         | Turb. journ. brg., flex. shoe                           | .513  | .482  | .150           | .395          | .459           |
| 4         | Turb. journ. brg., fixed shoe                           | .513  | .482  | .151           | .396          | .458           |
| 5         | Turb. end thrust brg.                                   | .503  | .467  | .148           | .380          | .433           |
| 6         | Compressor end thrust brg.                              | 0.492 | 0.467 | 0.150          | 0.381         | 0.432          |
| 7         | Comp. brg. mount  | .572  | .569  | .209           | .453          | .478           |
| 8         | Comp. brg. mount  | .554  | .569  | .210           | .433          | .469           |
| 9         | Comp. brg. mount  | .569  | .574  | .222           | .453          | .481           |
| 10        | Turb. brg. mount  | .544  | .379  | .150           | .385          | .437           |
| 11        | Turb. brg. mount  | 0.551 | 0.451 | 0.171          | 0.404         | 0.460          |
| 12        | Turb. brg. mount  | .528  | .502  | .205           | .420          | .464           |
| 13        | Turb. brg. mount  | .551  | .451  | .165           | .398          | .451           |
| 14        | Gimbal assembly   | ---   | .502  | .211           | .418          | .464           |
| 15        | Gimbal assembly   | ---   | .500  | .203           | .415          | .460           |
| 16        | Gimbal assembly   | ---   | 0.492 | 0.208          | 0.415         | 0.462          |
| 17        | Gimbal assembly   | ---   | .477  | .206           | .415          | .460           |
| 18        | Main frame assembly comp.<br>seal mounting flange       | .559  | .554  | ---            | .485          | .530           |
| 19        | Main frame assembly comp.<br>brg. carrier mount ring    | .533  | .538  | .234           | .434          | .482           |
| 20        | Main frame assembly turb.<br>brg. carrier mount ring    | .510  | .508  | .205           | .418          | .464           |
| 21        | Main frame assembly turb.<br>outer housing mount flange | 0.303 | 0.277 | 0.108          | 0.325         | 0.324          |
| 22        | Longeron  | .379  | .379  | .182           | .389          | .414           |
| 23        | Longeron  | .230  | .427  | .468           | .502          | .502           |
| 24        | Longeron  | .234  | .431  | .472           | .508          | .508           |
| 25        | Longeron  | .238  | .434  | .477           | .523          | .512           |
| 26        | Longeron  | 0.241 | 0.438 | 0.479          | 0.528         | 0.523          |
| 27        | Longeron  | .248  | .441  | .486           | .538          | .533           |
| 28        | Longeron  | .250  | .444  | .489           | .544          | .538           |
| 29        | Longeron  | .255  | .450  | .494           | .546          | .551           |
| 30        | Turb. seal assembly                                     | .049  | .274  | .278           | .169          | .205           |
| 31        | Turb. seal assembly                                     | 0.068 | 0.293 | 0.286          | 0.231         | 0.225          |
| 32        | Radiation shield  | .159  | .376  | .414           | ---           | .318           |
| 33        | Radiation shield  | .171  | .392  | .416           | ---           | .292           |

\*Original thermal map

\*\*Modified thermal map



Thermocouple locations for table 1 and 2

# SCHEMATIC DIAGRAM OF SOLAR BRAYTON CYCLE SYSTEM

ARGON WORKING FLUID

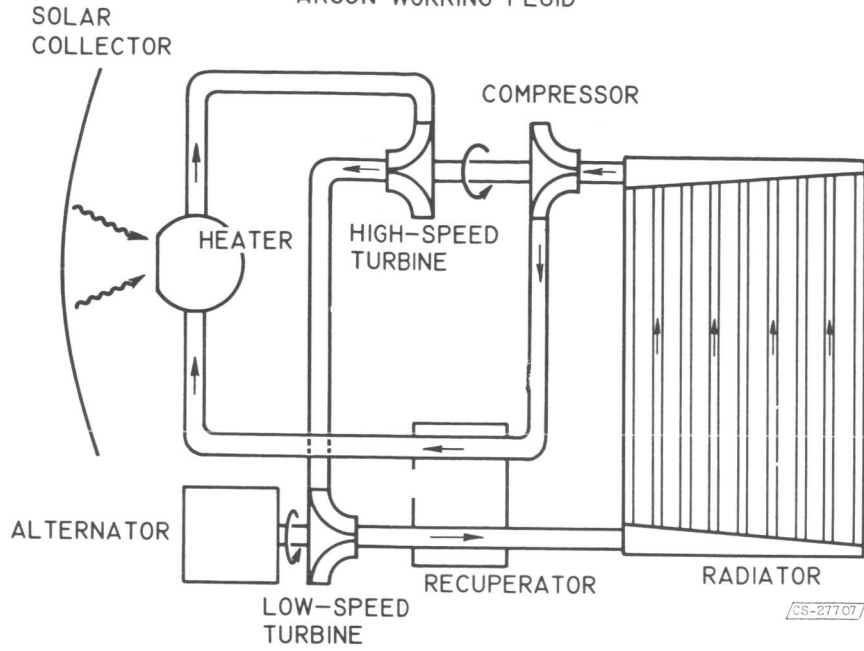


Figure 1

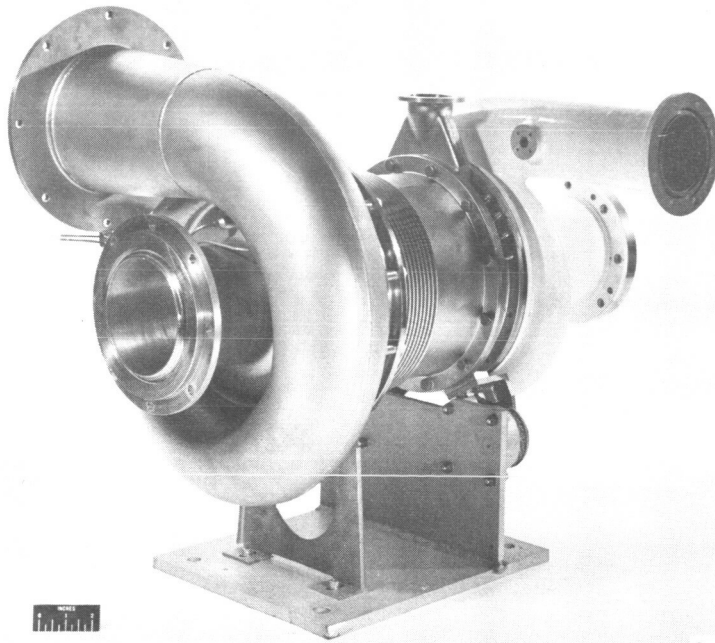


Figure 2. - Photograph of turbine-compressor package.

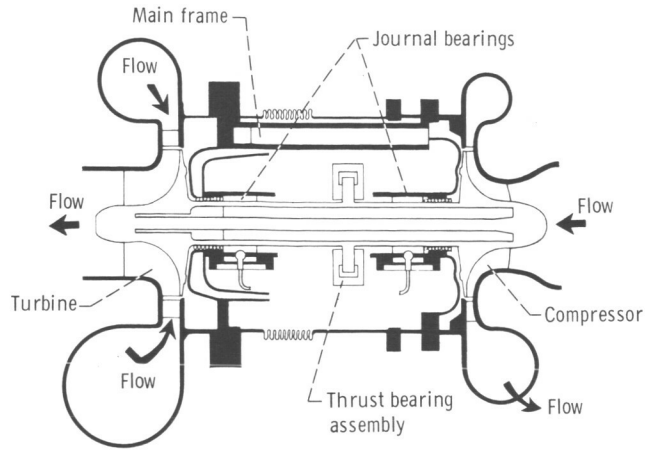
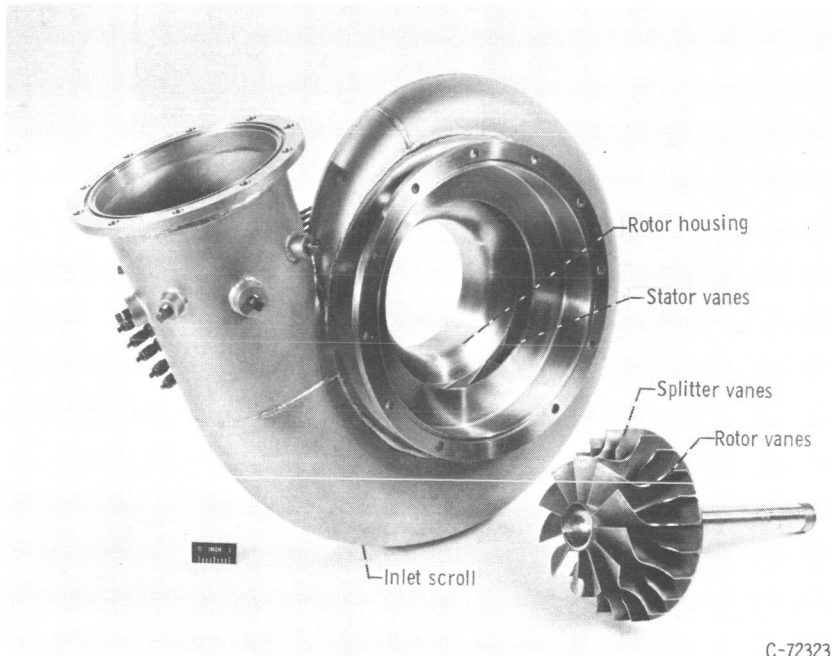


Figure 3. - Turbo-compressor package.



C-72323

Figure 4. - Turbine of turbine-compressor package.

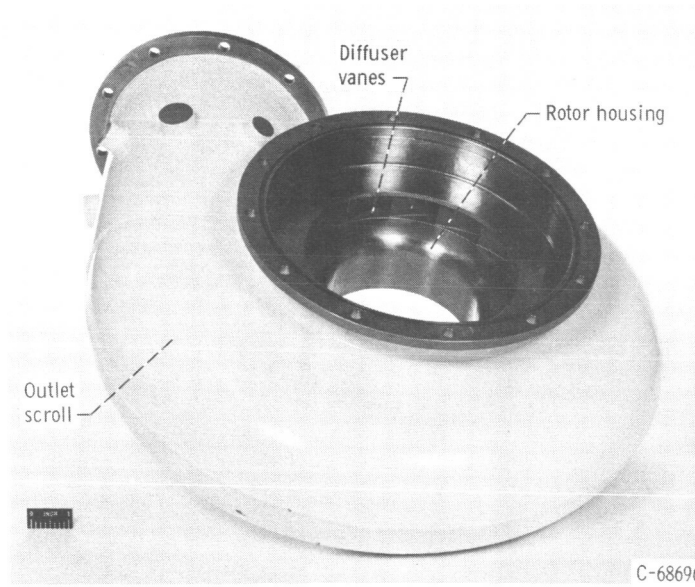
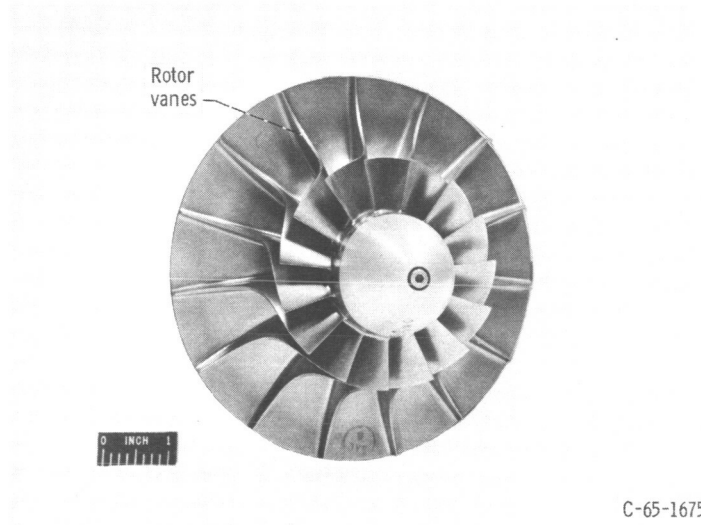
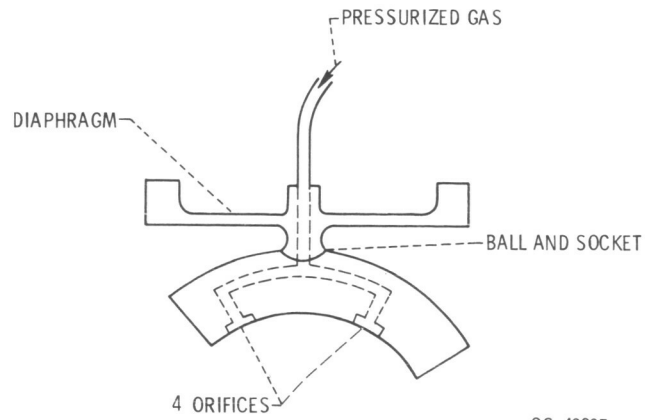


Figure 5. - Compressor of turbine compressor package.

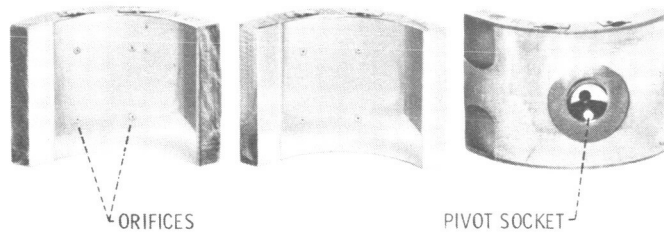
### PIVOT AND EXTERNAL PRESSURIZATION ARRANGEMENT



CS-40207

Figure 6(a)

### JOURNAL BEARING PADS



CS-40313

Figure 6(b)

### JOURNAL BEARING ARRANGEMENT

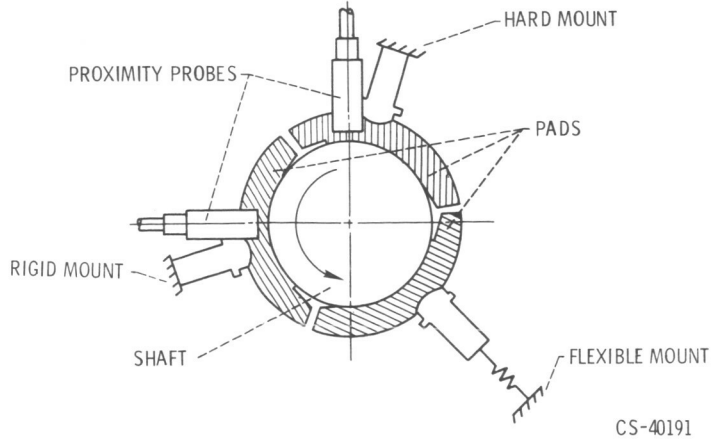
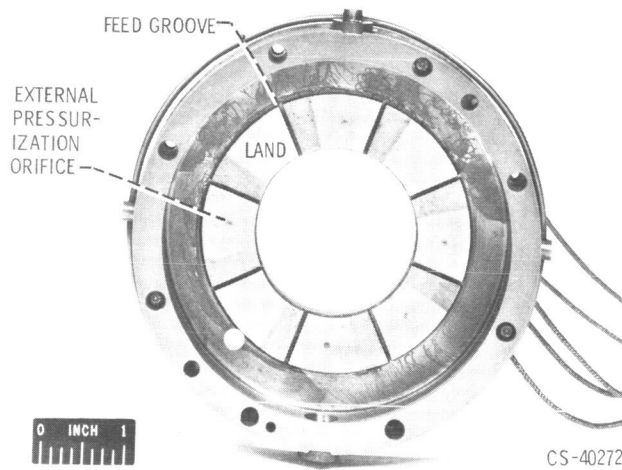


Figure 6(c)

CS-40191



CS-40272

Figure 7. - Rayleigh step thrust stator.

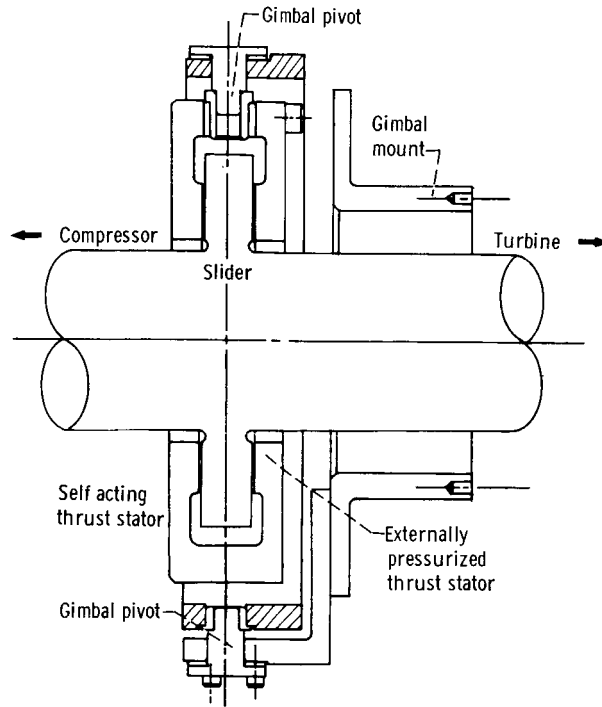


Figure 8. - Thrust bearing and gimbal assembly.

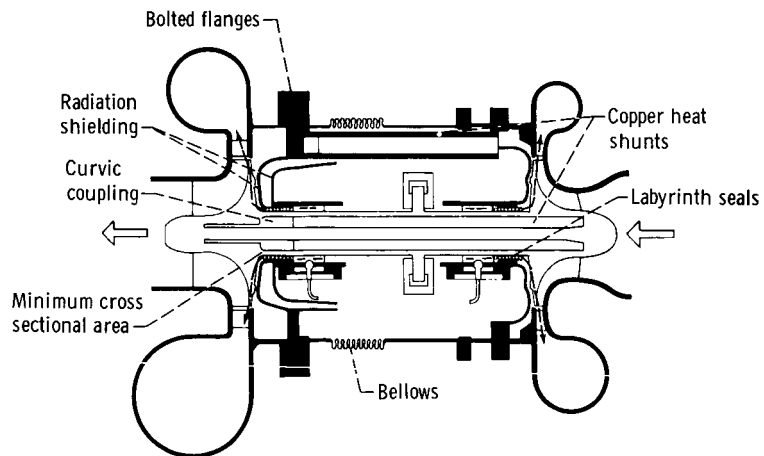


Figure 9. - Mechanical design features of turbo-compressor package.



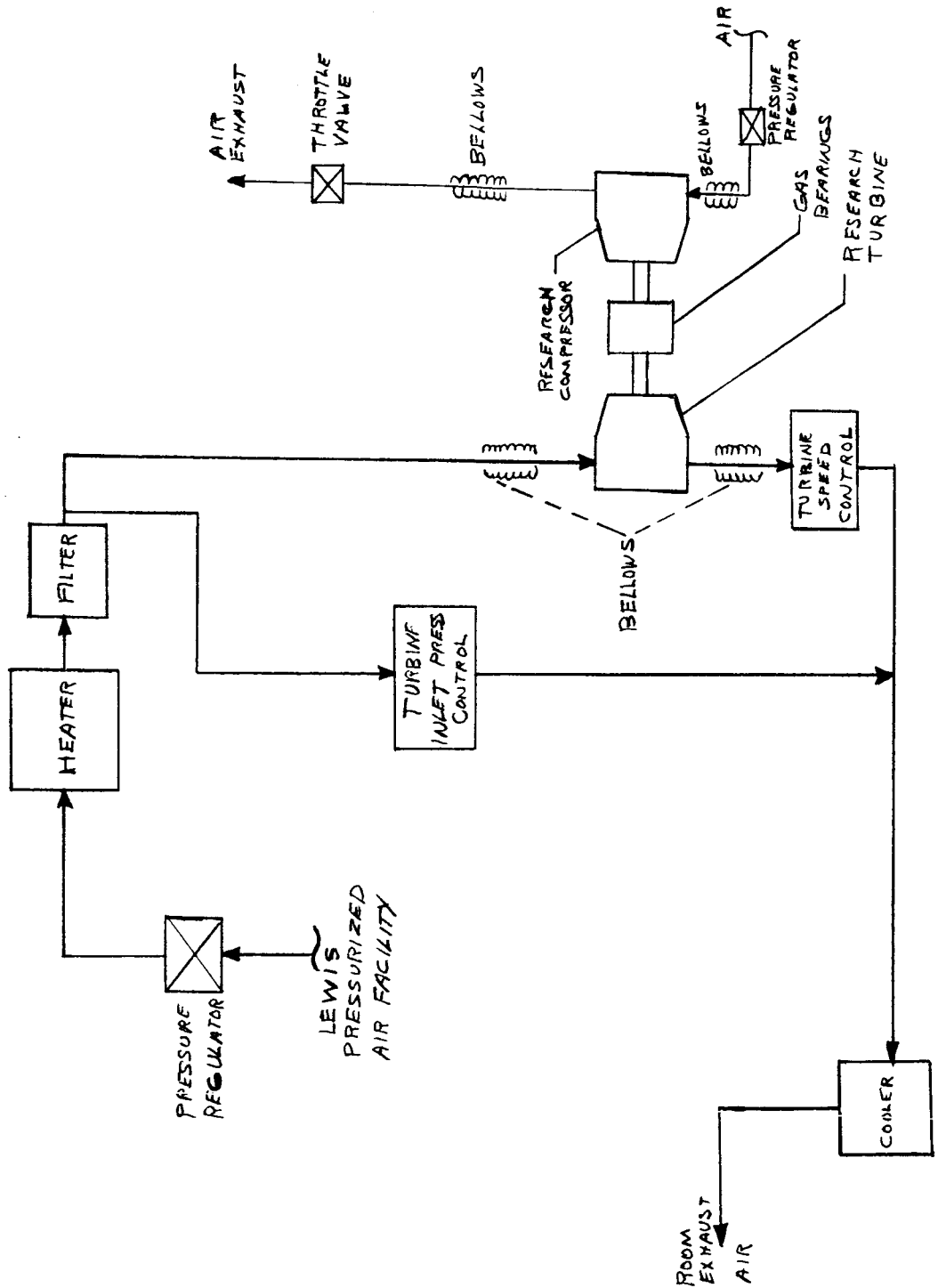


FIGURE 11 FLOW SCHEMATIC FOR TEST #1 OF PRELIMINARY INVESTIGATION OF TURBINE COMPRESSOR PACKAGE

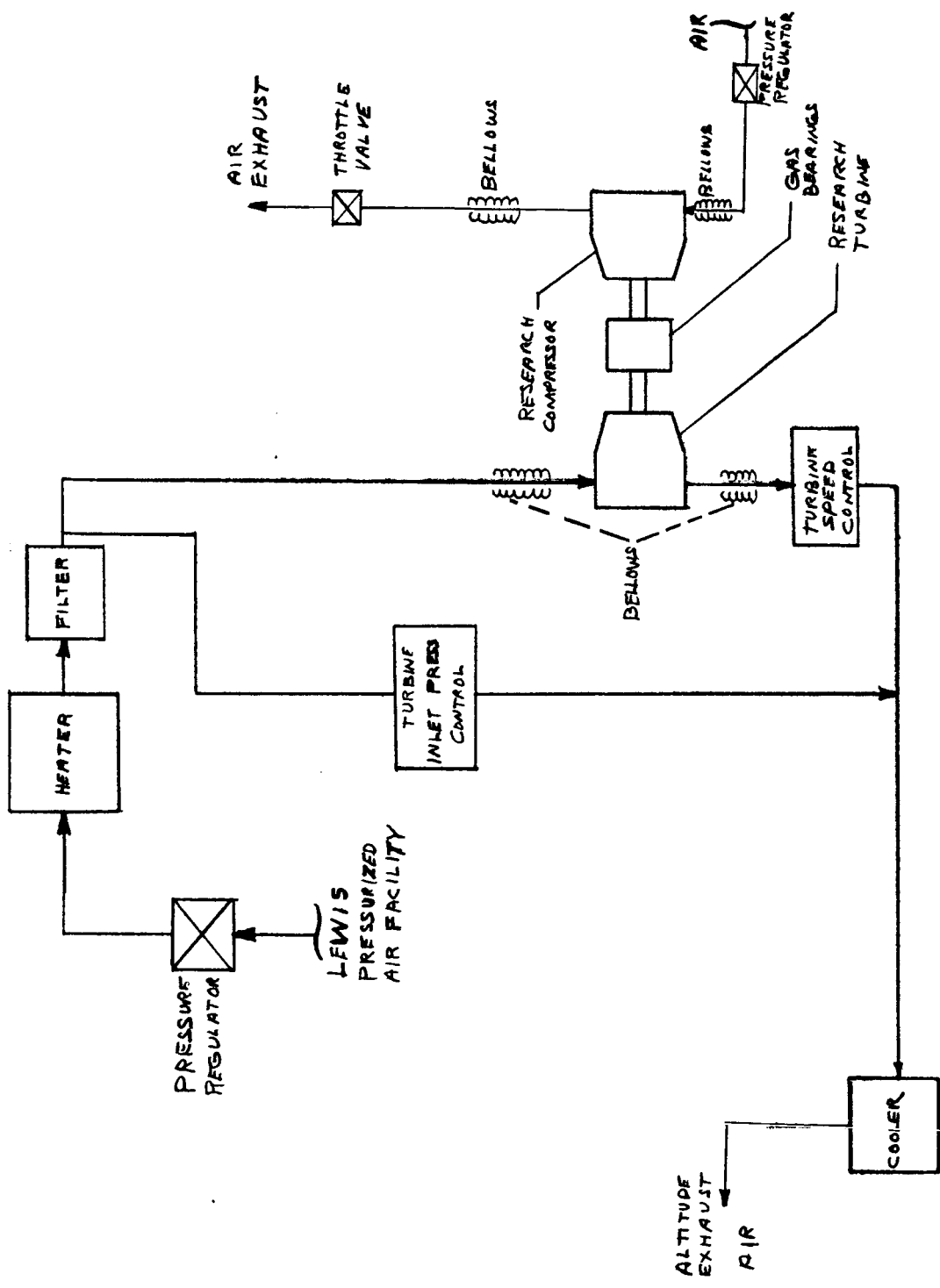
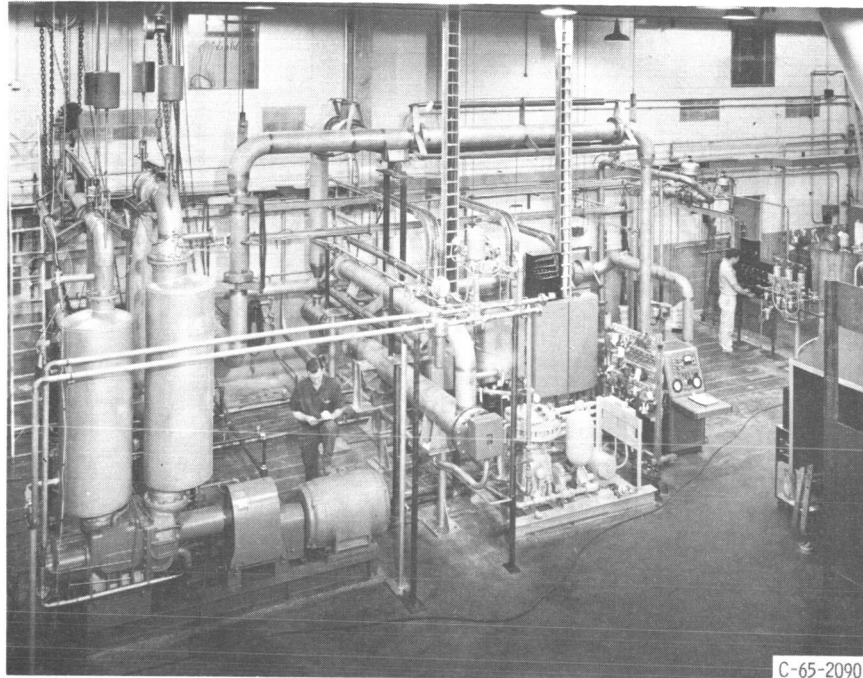
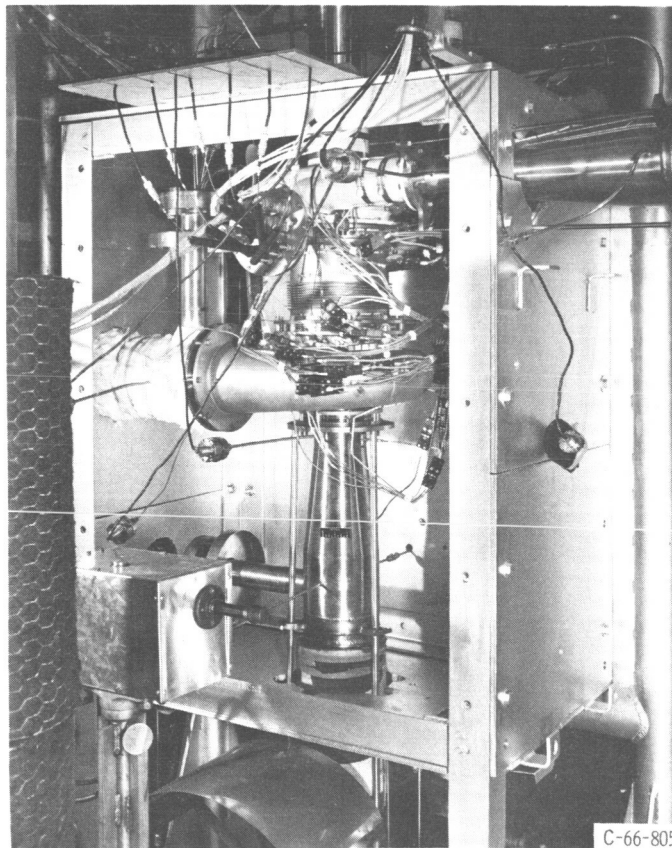


FIGURE 12 FLOW SCHEMATIC FOR TEST #2 OF PRELIMINARY INVESTIGATION OF TURBINE COMPRESSOR PACKAGE



C-65-2090

Figure 13. - Photograph of test facility.



C-66-805

Figure 14. - Photograph of turbocompressor installation.

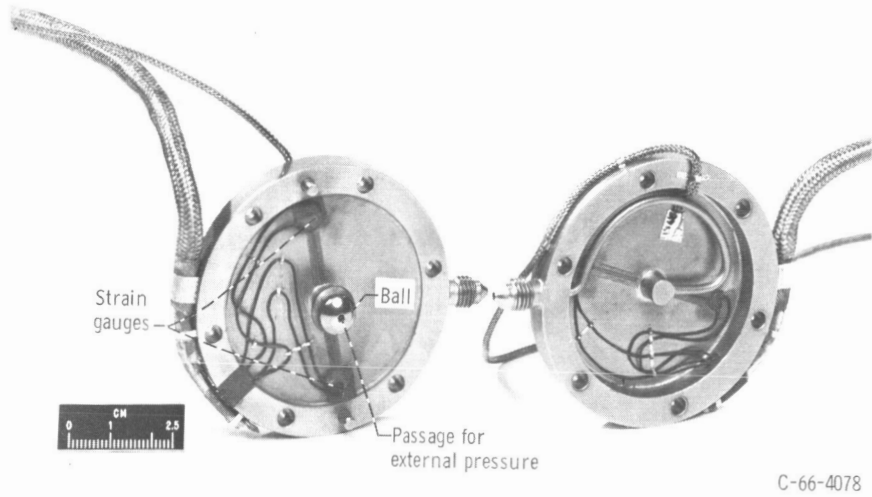


Figure 15. - Diaphragms showing strain gauges.

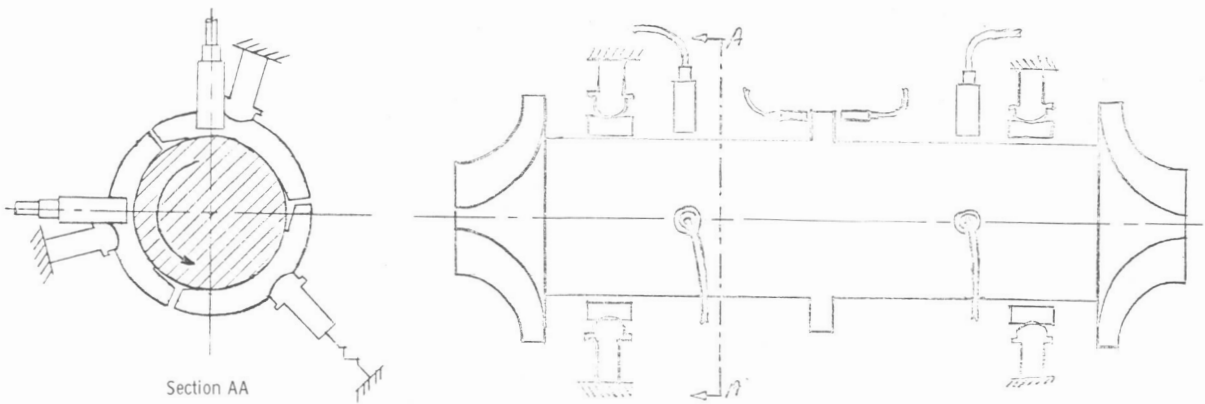
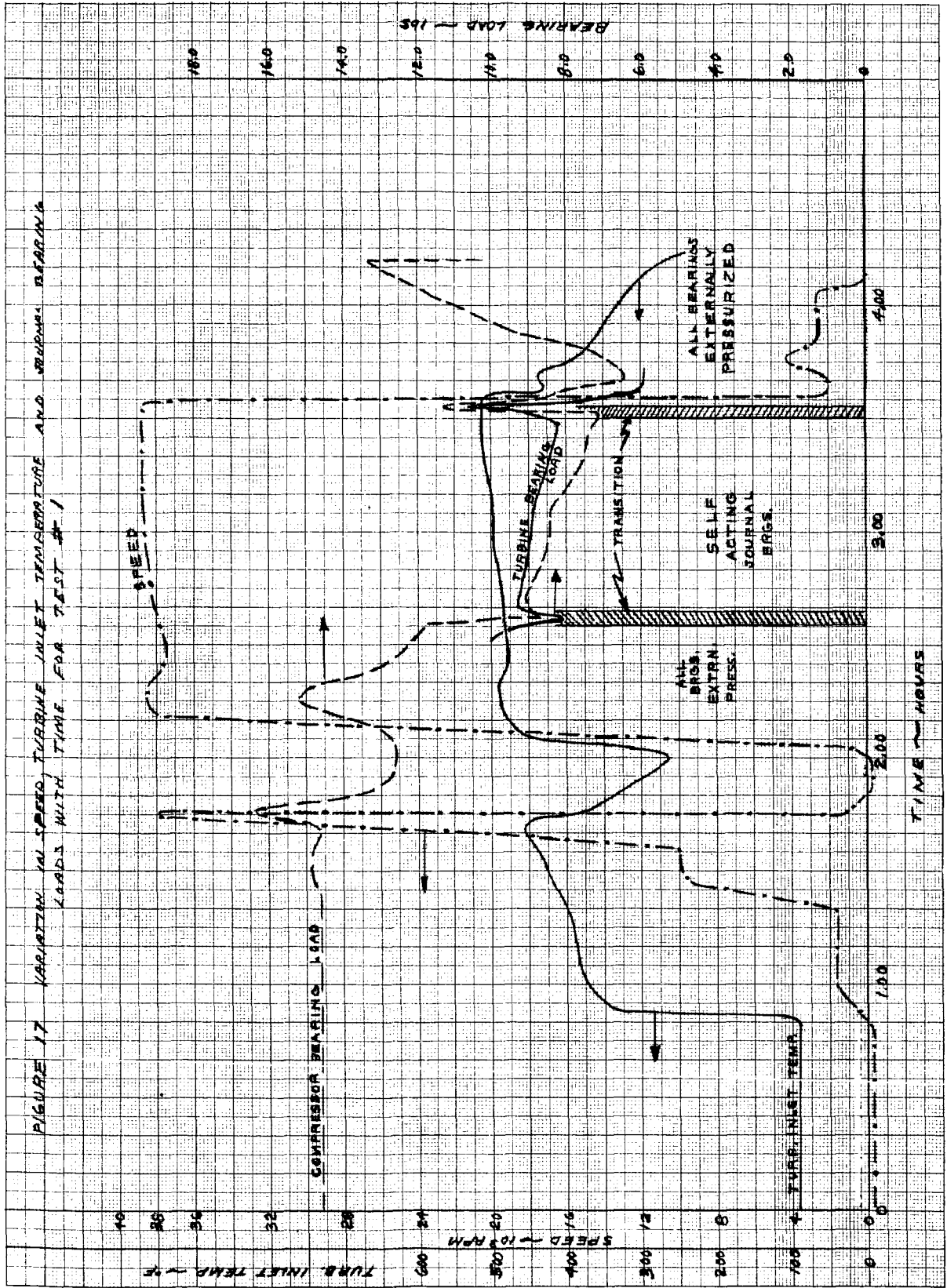


Figure 16. - Schematic of capacitance probe location.



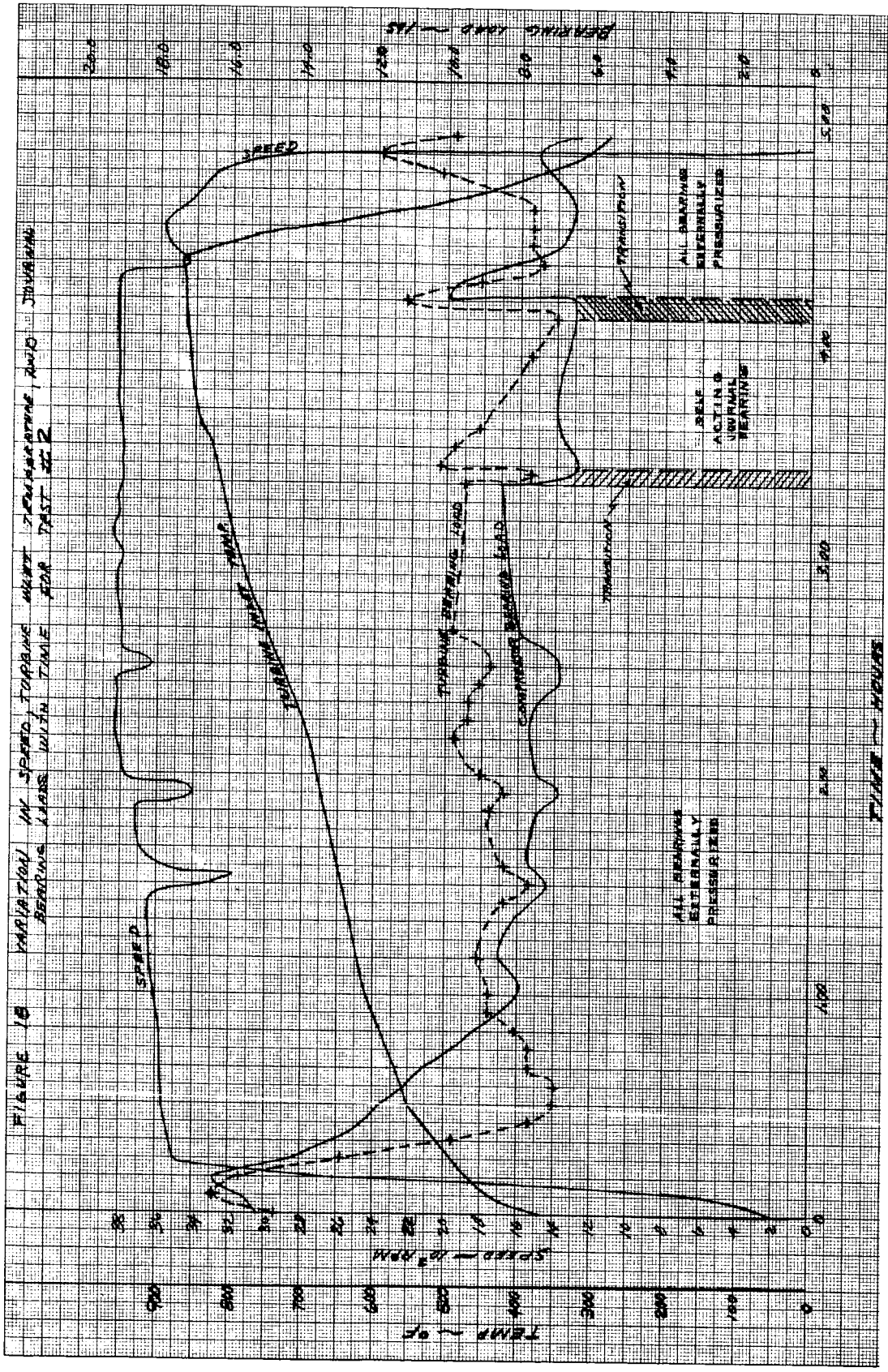
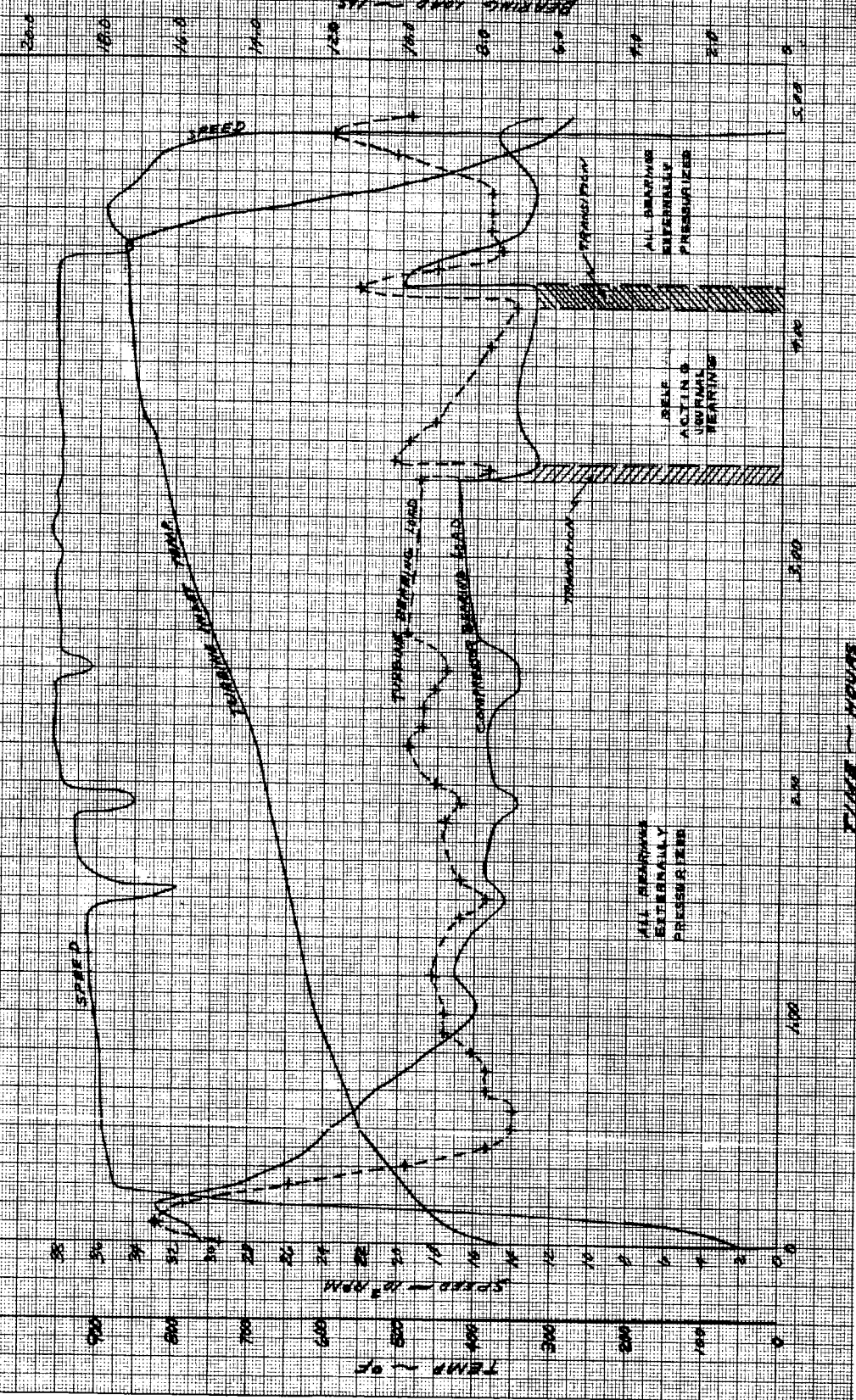
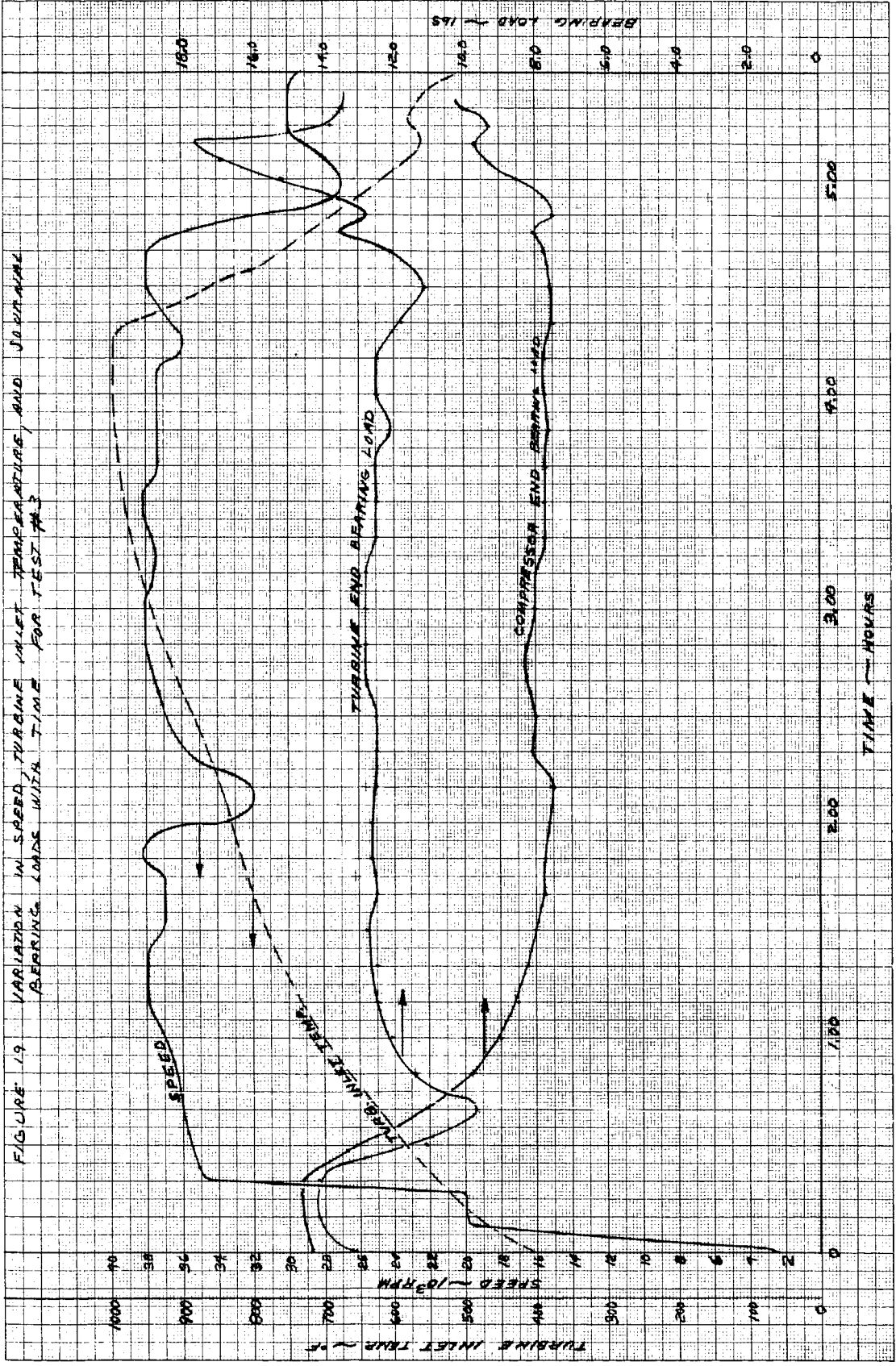


FIGURE 18 VARIATION IN SPEED, TORQUE, AND TEMPERATURE, AND TORQUE BEARING LOSS WITH TIME FOR TEST #2





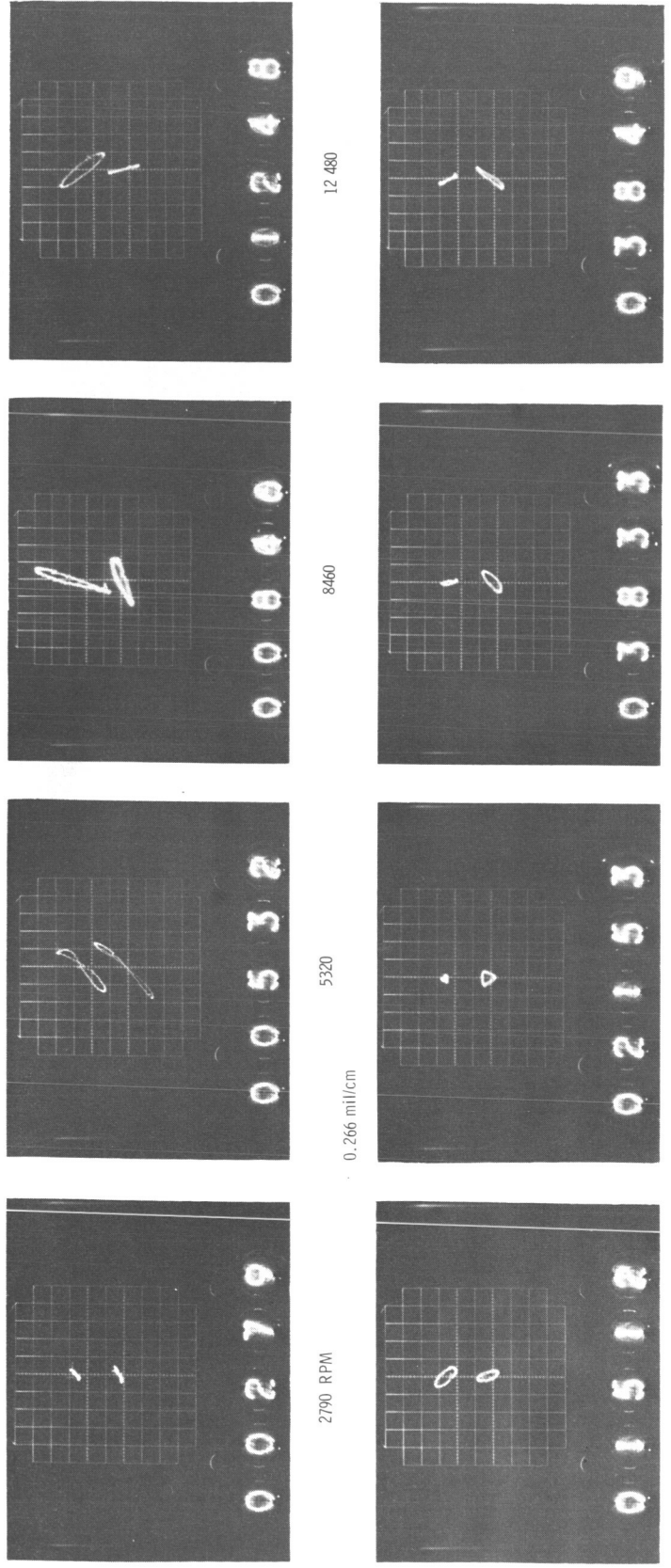


Figure 20. - Typical shaft orbits.

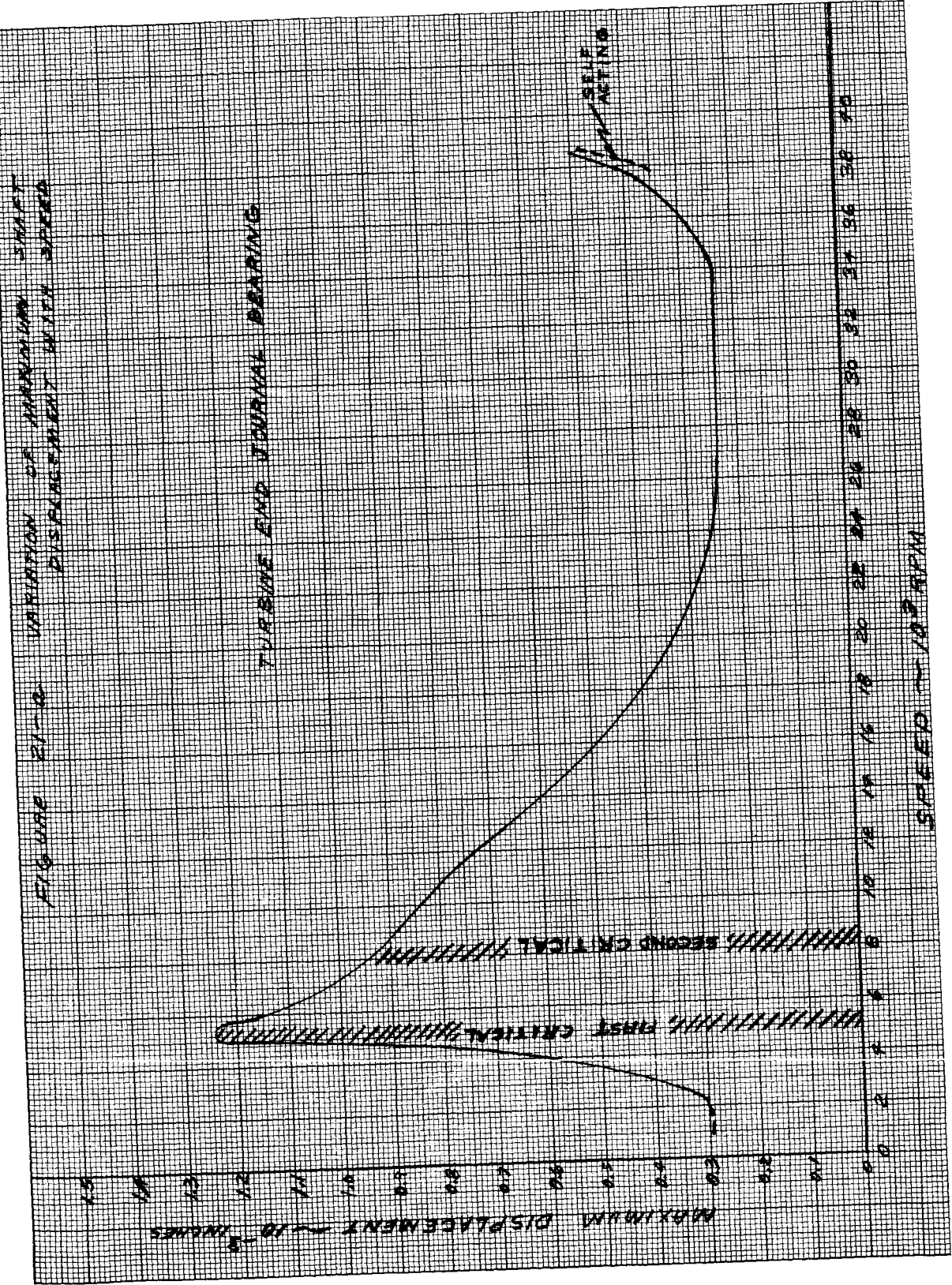


FIGURE 21--A VARIATION OF MAXIMUM SHAFT DISPLACEMENT WITH SPEED

